




Nitroreductase Increases Menadione-Mediated Oxidative Stress in *Aspergillus nidulans*

Yao Zhou,^a Hangya Lv,^a Haoxiang Li,^a Jingyi Li,^a Yunfeng Yan,^a Feiyun Liu,^a Wenliang Hao,^b Zheming Zhou,^b Ping Wang,^a
 Shengmin Zhou^a

^aState Key Laboratory of Bioreactor Engineering, School of Biotechnology, East China University of Science and Technology, Shanghai, People's Republic of China

^bKey Laboratory of Industrial Biotechnology (Ministry of Education), School of Biotechnology, Jiangnan University, Wuxi, Jiangsu, People's Republic of China

ABSTRACT Nitroreductases (NTRs) catalyze the reduction of a wide range of nitro-compounds and quinones using NAD(P)H. Although the physiological functions of these enzymes remain obscure, a tentative function of resistance to reactive oxygen species (ROS) via the detoxification of menadione has been proposed. This suggestion is based primarily on the transcriptional or translational induction of an NTR response to menadione rather than on convincing experimental evidence. We investigated the performance of a fungal NTR from *Aspergillus nidulans* (AnNTR) exposed to menadione to address the question of whether NTR is really an ROS defense enzyme. We confirmed that AnNTR was transcriptionally induced by external menadione. We observed that menadione treatment generated cytotoxic levels of O₂^{•-}, which requires well-known antioxidant enzymes such as superoxide dismutase, catalase, and peroxiredoxin to protect *A. nidulans* against menadione-derived ROS stress. However, AnNTR was counterproductive for ROS defense, since knocking out AnNTR decreased the intracellular O₂^{•-} levels, resulting in fungal viability higher than that of the wild type. This observation implies that AnNTR may accelerate the generation of O₂^{•-} from menadione. Our *in vitro* experiments indicated that AnNTR uses NADPH to reduce menadione in a single-electron reaction, and the subsequent semiquinone-quinone redox cycling resulted in O₂^{•-} generation. We demonstrated that *A. nidulans* nitroreductase should be an ROS generator, but not an ROS scavenger, in the presence of menadione. Our results clarified the relationship between nitroreductase and menadione-derived ROS stress, which has long been ambiguous.

IMPORTANCE Menadione is commonly used as an O₂^{•-} generator in studies of oxidative stress responses. However, the precise mechanism through which menadione mediates cellular O₂^{•-} generation, as well as the way in which cells respond, remains unclear. Elucidating these events will have important implications for the use of menadione in biological and medical studies. Our results show that the production of *Aspergillus nidulans* nitroreductase (AnNTR) was induced by menadione. However, the accumulated AnNTR did not protect cells but instead increased the cytotoxic effect of menadione through a single-electron reduction reaction. Our finding that nitroreductase is involved in the menadione-mediated O₂^{•-} generation pathway has clarified the relationship between nitroreductase and menadione-derived ROS stress, which has long been ambiguous.

KEYWORDS *Aspergillus nidulans*, menadione, nitroreductase, oxidative stress, ROS resistance

Reactive oxygen species (ROS) are by-products of aerobic metabolism generated endogenously from immune cells (1, 2), or exogenously by drug exposure (3–6). ROS include the superoxide anion (O₂^{•-}), hydrogen peroxide (H₂O₂), and hydroxyl radicals (OH•), all of which confer reactivity to different biological targets such as lipids,

Citation Zhou Y, Lv H, Li H, Li J, Yan Y, Liu F, Hao W, Zhou Z, Wang P, Zhou S. 2021. Nitroreductase increases menadione-mediated oxidative stress in *Aspergillus nidulans*. *Appl Environ Microbiol* 87:e01758-21. <https://doi.org/10.1128/AEM.01758-21>.

Editor Haruyuki Atomi, Kyoto University

Copyright © 2021 American Society for Microbiology. All Rights Reserved.

Address correspondence to Shengmin Zhou, zhoushengmin@ecust.edu.cn.

Received 10 September 2021

Accepted 30 September 2021

Accepted manuscript posted online 6 October 2021

Published 24 November 2021

proteins, and DNA. In both prokaryotic and eukaryotic organisms, high levels of oxidative stress generated by intracellular ROS are involved in many pathological processes, damaging living cells (2, 7). Therefore, investigations into cell sensitivity, adaptivity, and resistance to cytotoxic ROS are important.

Most studies of oxidative stress at the molecular level have used free-radical-generating compounds. Menadione (2-methyl-1,4-naphthoquinone) is a useful $O_2^{\bullet-}$ generator due to its water solubility and ease of diffusion (8, 9). Menadione appears to generate ROS by reducing one-electron quinone to semiquinone (9, 10). The semiquinone is then autoxidized back to quinone under aerobic conditions. The by-product of this reaction is $O_2^{\bullet-}$. In biological systems, quinones are generally reduced by coenzyme NAD(P)H in the presence of cellular reductases, including NADH ubiquinone oxidase, NADH cytochrome b_5 reductase, and NADPH cytochrome P-450 reductase (10). These three reductases therefore appear to be responsible for the generation of ROS by menadione.

Nitroreductases are a family of evolutionarily related proteins involved in reducing nitroaromatic and nitroheterocyclic compounds using flavin adenine dinucleotide (FAD) or flavin mononucleotide (FMN) as the cofactor and NAD(P)H as a reducing equivalent (11). Bacterial nitroreductases can be classified as oxygen insensitive (type I) or oxygen sensitive (type II) according to their biochemical characteristics (11). The oxygen-insensitive nitroreductases catalyze the two-electron reduction of nitro-compounds to produce nitroso and hydroxylamine and finally primary amines. The oxygen-sensitive nitroreductases catalyze the one-electron reduction of nitro groups to form a nitro anion radical, which subsequently reacts with oxygen, producing $O_2^{\bullet-}$ and regenerating the initial nitro-compound. As well as reducing nitro-compounds, nitroreductases have been shown to be efficient quinone reductases. Oxygen-insensitive bacterial nitroreductases have been reported to reduce lawsone to its hydroquinone, which can function as a redox mediator in the subsequent reduction of azo compounds outside the cells (12). Therefore, bacterial nitroreductases have received considerable attention because they can be used for the biodegradation of environmental pollutants (11). However, these compounds may not be the physiological substrates of nitroreductases because they are the products of human activities. The real physiological functions of nitroreductases remain obscure.

Some studies have shown that nitroreductases may be involved in the response to anti-oxidative stress. Bacterial nitroreductases, which include *nfsA* in *Escherichia coli* (13, 14), *snrA* in *Salmonella enterica* serovar Typhimurium, and *nprA* in *Rhodobacter capsulatus* are induced at high levels by the oxidant-producing herbicide paraquat (13–15). In *Saccharomyces cerevisiae*, disruption of two nitroreductases, *Frm2p* and *Hbn1p*, increased the sensitivity of yeast to nitro-compound-derived oxidative stress (16). However, the definitive conclusion that nitroreductases (NTRs) are antioxidants could not be drawn only from these transcriptional and phenotypic findings. Another indication that nitroreductases are involved in defense against oxidative stress is the observation that the deazaflavin-dependent nitroreductase from *Mycobacterium tuberculosis* protects mycobacteria from oxidative stress by catalyzing the two-electron reduction of menadione to less-toxic hydroquinone, competing with the one-electron reduction pathway to avoid $O_2^{\bullet-}$ formation (17). However, deazaflavin-dependent nitroreductase is a special case among nitroreductases and only spreads in a few species of archaea and bacteria (17, 18). In fungi, one of the *Aspergillus nidulans* nitroreductase-like proteins, AnNTR (encoded by *AN2343*), was identified and shown to be significantly induced under menadione-mediated oxidative stress conditions (19–21). However, it is not clear whether fungal nitroreductase really plays a role in antioxidative stress because the effect on menadione resistance of deleting this gene was not investigated.

Filamentous fungi are important in industry, having important roles in pharmacology and medicine. Fungi frequently encounter high levels of oxidative stress, generated by host-pathogen defense and fermentation (22, 23). *A. nidulans* is an excellent model fungus with which to study such important processes in genetics and cell biology. Therefore, the elucidation of a novel antioxidant system in *A. nidulans* is valuable, both

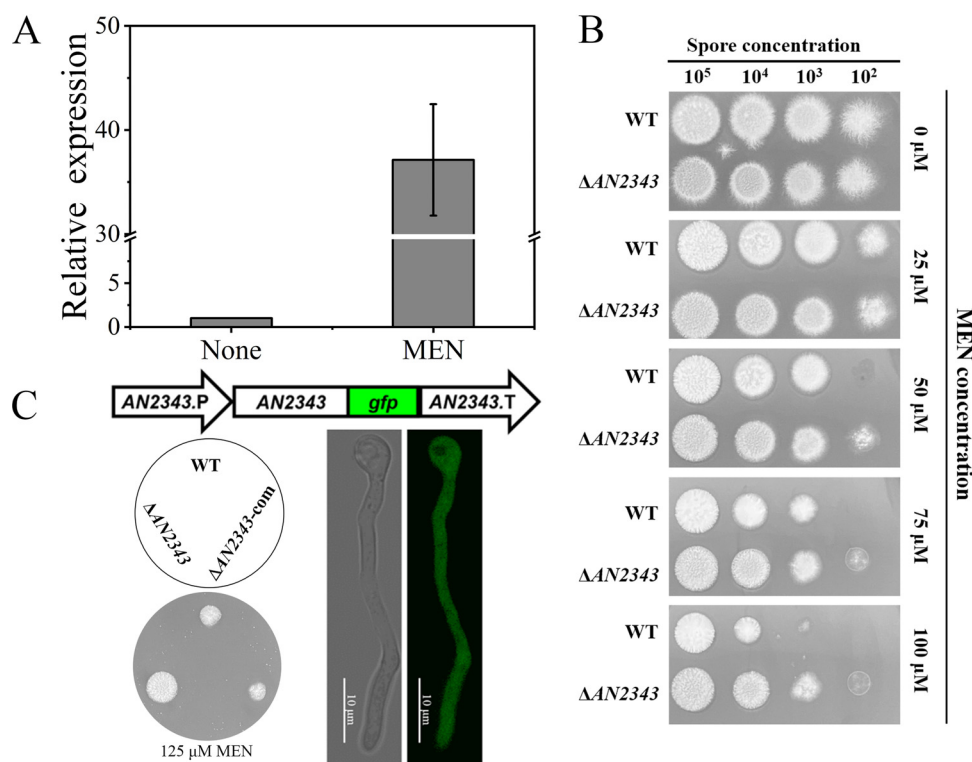


FIG 1 Response of *AN2343* to external menadione. (A) Q-RT-PCR analysis of *AN2343* induced by menadione. After preculture for 16 h, the WT strain was exposed to 0.8 mM menadione (MEN) for 3 h. The relative mRNA levels were normalized to that of *actA*. Error bars represent the standard deviations (SD) of three independent experiments. (B) Deleterious effect of AnNTR on protection against menadione. After incubation of *A. nidulans* conidiospores on agar plates containing various concentrations of menadione at 37°C for 48 h, the colony morphology was examined to determine the sensitivities to menadione. (C) Recovery of menadione sensitivity by the expression of AnNTR-GFP in $\Delta AN2343$ and the subcellular localization of AnNTR-GFP. The AnNTR::GFP fusion protein was expressed using the native promoter and terminator of *AN2343*. Conidiospores (1×10^5) from the WT, $\Delta AN2343$, and $\Delta AN2343$ -com ($\Delta AN2343$ complemented with AnNTR-GFP) strains were cultivated on minimal medium agar plates supplemented with 125 μ M MEN at 37°C for 48 h. The fluorescence from strains cultivated in liquid MM without menadione for 16 h was observed by using confocal laser scanning microscopy.

because it provides a deeper understanding of the biology of this important group of organisms and because of the potential industrial and medical applications that may arise from this work.

According to the current literature, *A. nidulans* nitroreductase appears to play a direct role in resisting menadione-derived oxidative stress. However, when we characterized the phenotype of the *AN2343* deletion mutant, we found that a deficiency of *AN2343* instead enhanced the strain's resistance to menadione. That observation triggered our current effort to investigate in depth the mechanisms underlying the promotion of menadione-mediated cytotoxicity by AnNTR.

RESULTS

AnNTR had a deleterious effect on protection against menadione. The nitroreductase-like protein AnNTR, which is encoded by *AN2343*, has been identified as a protein induced in menadione-exposed *A. nidulans* cells (20, 21). However, there is no evidence for the involvement of *AN2343* in protection against oxidative stress. To investigate the relationship between AnNTR and oxidative stress, we investigated the transcription profile of *AN2343* in response to exposure to external menadione. *AN2343* expression was significantly induced by 0.8 mM menadione (Fig. 1A), suggesting the possibility that *AN2343* is involved in menadione metabolism. We deleted *AN2343* to examine the disrupted strain's sensitivity to oxidative stress induced by menadione and H₂O₂. There was no detectable

difference in growth between $\Delta AN2343$ and the control strain (wild type [WT]) (Fig. 1B) under normal conditions. Menadione was toxic to both strains in a dose-dependent manner. However, the deletion of *AN2343* appeared to relieve the cytotoxicity caused by menadione (Fig. 1B). The application of 75 μM menadione inhibited the cell growth of WT more strongly than that of $\Delta AN2343$, and the difference was amplified when the concentration of menadione was increased to 100 μM . Subsequent reintroduction of *AN2343* fused with green fluorescent protein (GFP; $\Delta AN2343$ -com), flanked by its native promoter and terminator, restored the sensitivity to menadione compared to the WT (Fig. 1C), confirming the adverse function of AnNTR in the detoxification of menadione. The function of AnNTR-GFP, as well as the whole-cell fluorescence imaging described in Fig. 1C, indicated that AnNTR is localized to the cytosol. In a control experiment, *AN2343* did not increase H_2O_2 damage because the deletion of *AN2343* did not affect the sensitivity of the strain to H_2O_2 (see Fig. S2A). These observations do not support the proposition that AnNTR may act as an antioxidant enzyme that protects the cell against menadione toxicity but suggested an opposing hypothesis: that AnNTR may be involved in the conversion of menadione to toxic metabolites in *A. nidulans*.

Disruption of *AN2343* decreased intracellular $\text{O}_2^{\bullet-}$ derived from menadione. As an $\text{O}_2^{\bullet-}$ -producing agent, menadione is believed to trigger cellular oxidative stress. However, its physiological effects may be more extensive. For example, it may destroy cellular 4Fe-4S proteins, resulting in the production of deleterious OH^\bullet radicals (24), and directly affecting the GSH pool of cells (25). It may also chemically modify cell components (26), generating nonoxidative stress in cells. The question of whether $\text{O}_2^{\bullet-}$ originating from menadione results in cytotoxicity has not been addressed experimentally. We quantified the menadione-derived intracellular $\text{O}_2^{\bullet-}$ using dihydroethidium (DHE), a membrane-permeable probe that reacts with $\text{O}_2^{\bullet-}$ to form the highly fluorescent ethidium cation. In the absence of menadione, there was only weak fluorescence when the cells were loaded with DHE (Fig. 2A). The fluorescence was completely quenched when the ROS scavenger *N*-acetyl-L-cysteine (NAC; 10 mM) was applied, indicating the existence of a small amount of intracellular $\text{O}_2^{\bullet-}$ production (Fig. 2A), a by-product of cellular respiration under normal physiological conditions (27). The application of 300 μM menadione induced a significant rise in fluorescence, and the menadione-induced elevation of ROS was completely prevented by the presence of NAC (Fig. 2A). These results provide evidence for the generation of $\text{O}_2^{\bullet-}$ in response to menadione. We estimated the oxidative stress level caused by menadione by observing the phenotypes of *sodA*, *prxA*, and *catB* deletion mutants on menadione-containing plates because the fungus generally eliminates ROS using these well-known antioxidants. The gene *sodA* encodes a copper-zinc superoxide dismutase, the key $\text{O}_2^{\bullet-}$ dismutase responsible for superoxide dismutation during oxidative stress (28). The genes *prxA* and *catB* encode a key peroxiredoxin and a major catalase, respectively, and are indispensable for defense against H_2O_2 (29–31). Compared to the WT phenotype, the growth of cells treated with concentrations of menadione as low 50 μM was significantly inhibited (Fig. 2B). The growth of $\Delta sodA$ cells under menadione concentrations of 100 μM was completely blocked. Menadione also inhibited $\Delta prxA$ and $\Delta catB$ strains in a dose-dependent manner (Fig. 2B). This observation indicated that ROS induced by menadione, including $\text{O}_2^{\bullet-}$ and its decomposition product H_2O_2 , produced considerable oxidative stress in cells.

There are two plausible mechanisms for the way in which AnNTR could increase menadione-mediated oxidative stress in *A. nidulans*: (i) suppression of the expression of ROS resistant genes and (ii) direct involvement in menadione-derived ROS generation. We compared the transcriptional profiles of the ROS resistance genes, including *sodA*, *catB*, and *prxA*, in response to menadione in WT and $\Delta AN2343$ strains (see Fig. S3). Treatment with 0.8 mM external menadione induced the expression of all of these genes to different extents, without obvious differences between the WT and $\Delta AN2343$ strains. This finding appears to exclude the possibility that AnNTR participates in the transcriptional regulation of ROS resistance genes. To investigate whether AnNTR is directly involved in menadione-dependent $\text{O}_2^{\bullet-}$ production in *A. nidulans* cells, we

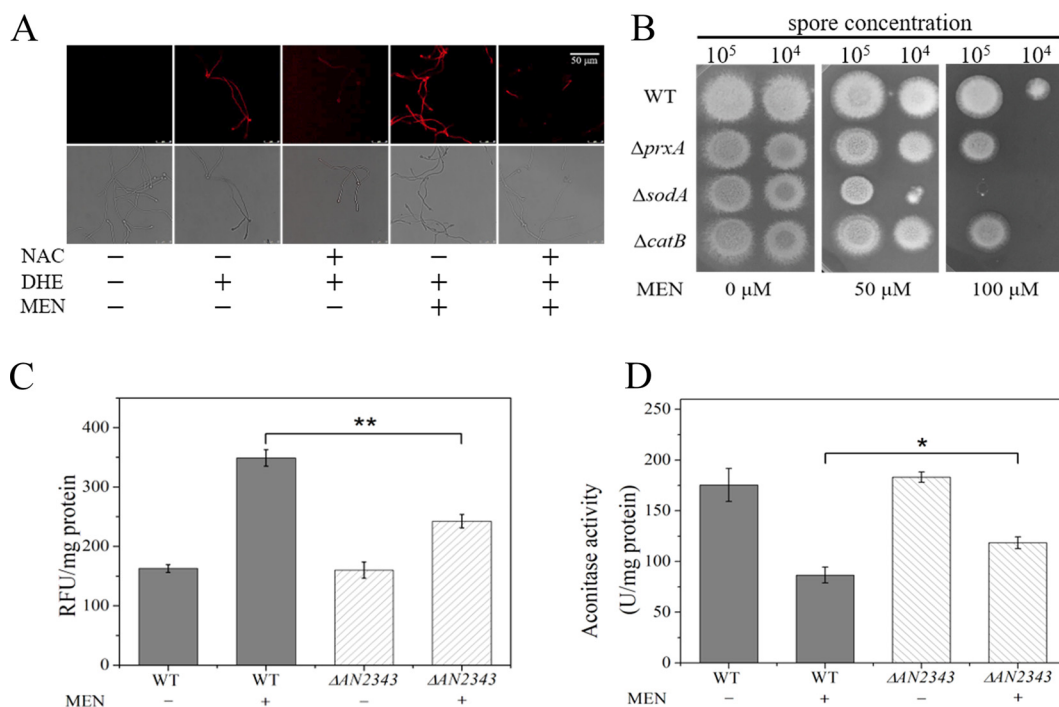


FIG 2 AnNTR is an efficient $O_2^{\bullet-}$ -producing enzyme in *A. nidulans* in the presence of menadione. (A) Images of intracellular $O_2^{\bullet-}$ levels using an $O_2^{\bullet-}$ specific fluorescent probe. After 12 h of cultivation, the strains were treated with or without menadione (MEN; 300 μ M), followed by incubation with 10 μ M dihydroethidium (DHE) for another 30 min, and then observed using fluorescence microscopy. The $O_2^{\bullet-}$ scavenger NAC (10 mM) was added to block $O_2^{\bullet-}$ generation as a control experiment. (B) ROS-resistant enzymes were involved in the menadione stress defense. Conidia from WT, $\Delta prx A$, $\Delta sod A$, and $\Delta cat B$ strains were spotted onto MM plates with or without the indicated concentrations of menadione, followed by incubation at 37°C for 48 h. (C) Effects of *AN2343* deletion on intracellular $O_2^{\bullet-}$ generation. After 16 h of cultivation, the mycelia of the WT and $\Delta AN2343$ strains were exposed to 0.8 mM menadione for another 6 h, followed by a further 1 h of incubation with DHE (10 μ M). Mycelia were disrupted by grinding in liquid nitrogen, and the fluorescence in the supernatant was measured. Values (means \pm the SD of three independent experiments) represent relative fluorescence units (RFU) per mg of total cell protein. (D) Menadione-induced cellular oxidative damage is reflected by the inhibition of the activity of intracellular aconitase. After menadione treatment, the mycelia of the WT and $\Delta AN2343$ strains were disrupted, and the activities in the cell extracts were measured. The data are the means \pm the SD of three independent experiments. One-way ANOVA was used to test for significant differences among the means (*, $P < 0.05$; **, $P < 0.01$).

compared the changes in intracellular $O_2^{\bullet-}$ levels before and after exposure of WT and $\Delta AN2343$ strains to menadione by measuring the fluorescence intensity of DHE. We found that the absence of AnNTR did not change $O_2^{\bullet-}$ accumulation under non-stressed conditions but decreased the level of $O_2^{\bullet-}$ by one-third compared to that of the WT under menadione stress conditions (Fig. 2C), suggesting that AnNTR is an efficient menadione-dependent $O_2^{\bullet-}$ generator in *A. nidulans*.

We estimated the extent of oxidative damage to cells caused by $O_2^{\bullet-}$ derived from menadione converted by AnNTR. Aconitase is a major target of ROS because of its particularly sensitive 4Fe-4S cluster (32). No difference in cellular aconitase activity was observed between WT and $\Delta AN2343$ cells under normal conditions (Fig. 2D). Treatment with 0.8 mM menadione inhibited the activity of cellular aconitase in the WT to a greater extent than in the $\Delta AN2343$ strain (Fig. 2D), indicating that menadione-derived $O_2^{\bullet-}$ converted by AnNTR led to substantial cellular oxidative damage in *A. nidulans*.

Recombinant AnNTR exhibited menadione reductase activity. To investigate the mechanisms by which AnNTR catalyzes the generation of $O_2^{\bullet-}$ from menadione, we expressed and purified recombinant AnNTR using an *E. coli* expression system. AnNTR can only be produced successfully in the *E. coli* thioredoxin N-terminal tagged form (AnNTR-Trx, 35 kDa) (see Fig. S4A). After purification, the Trx tag was removed from the recombinant protein to facilitate analysis of its activity. To indicate the occurrence of

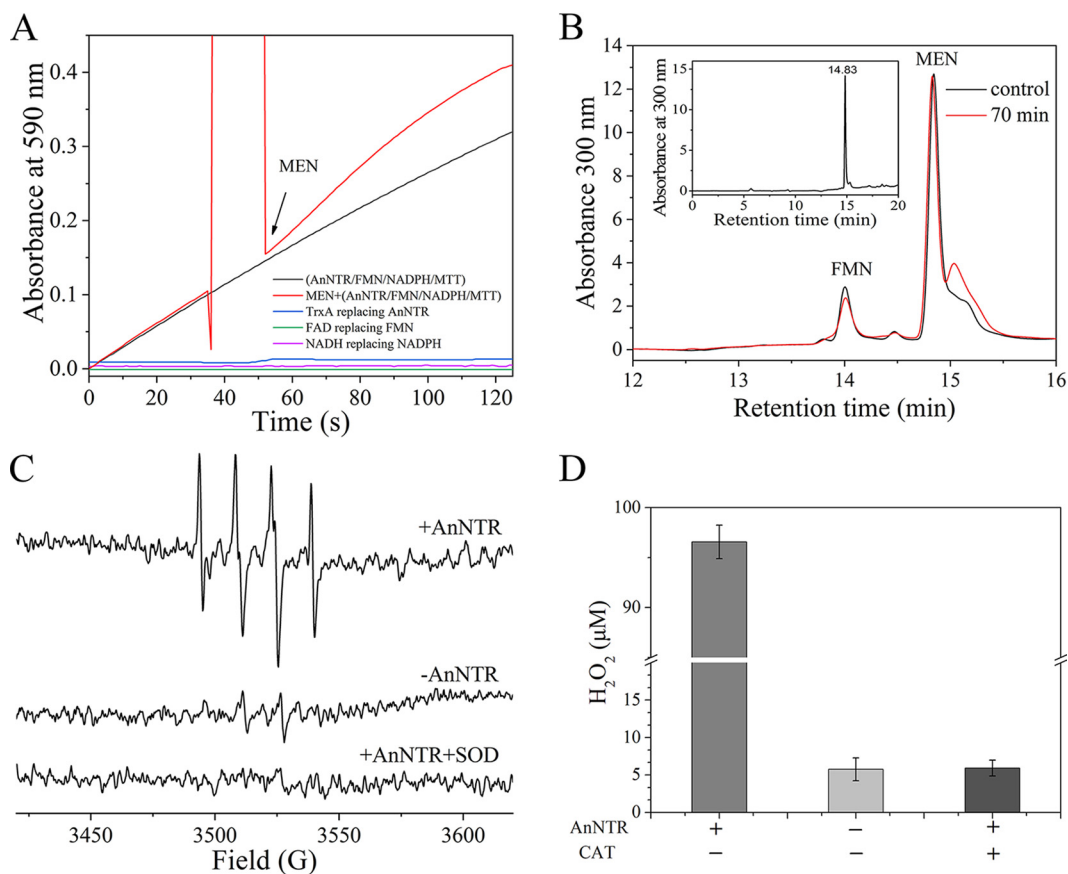


FIG 3 AnNTR drives the one-electron metabolism of menadione, leading to ROS generation via redox cycling. (A) Reduction activity of recombinant AnNTR toward menadione. MTT was used as the ultimate electron acceptor of menadione reduction, and the MTT reduction product formazan was measured at 590 nm to measure the reduction due to menadione. The reaction mixture was 0.5 ml of sodium phosphate buffer (50 mM [pH 7.4]), NADPH (100 μ M), DTPA (100 μ M), FMN (10 μ M), MTT (0.5 mM), and AnNTR (1.5 μ g). The arrow indicates the time point of menadione (MEN; 50 μ M) addition. As three controls, TrxA (2.6 μ g) replacing AnNTR, NADH (100 μ M) replacing NADPH, and FAD (10 μ M) replacing FMN were added to the reaction solution in the presence of menadione. (B) No changes in menadione concentration were observed before or after menadione reduction catalyzed by AnNTR. After incubation for 70 min at 25°C, the reaction mixture was analyzed by using HPLC. The mixture without AnNTR was the control. (C) Confirmation of $O_2^{\bullet-}$ generation during menadione reduction procedure by EPR spectroscopy. DMPO was used as an $O_2^{\bullet-}$ trapper, and the four successive peaks are the characteristic spectrum of a DMPO- $O_2^{\bullet-}$ adduct. EPR spectra of the spin adduct of the reaction mixture obtained in the absence or presence of AnNTR or AnNTR plus SOD are shown. (D) H_2O_2 generation during the menadione reduction procedure. H_2O_2 was measured using hydrogen peroxide assay kits, and the absorbance was measured at 540 nm. Catalase (CAT) was employed to eliminate H_2O_2 in the reaction solution. The data are the means \pm the SD of three independent experiments.

the reduction reaction, we used a functional assay based on the reduction of MTT to formazan by reduced substrates (33). Formazan has a characteristic absorption peak at 590 nm. Using NADPH as an electron donor, we found that, in the absence of menadione, the addition of FMN, but not FAD, resulted in a significant increase in absorbance at 590 nm (Fig. 3A). Under the same reaction conditions, NADH did not produce any change in absorbance (Fig. 3A). These findings indicate that AnNTR is an efficient NADPH-dependent FMN reductase. Adding menadione to the existing reaction solution further promoted the generation of formazan (Fig. 3A). Replacing AnNTR with its protein tag TrxA did not facilitate dye generation, excluding the possibility that trace amounts of TrxA were involved in the reaction as a purification contaminant (Fig. 3A). These results indicated that menadione is a good substrate for AnNTR when NADPH is used as an electron donor and FMN as a cofactor.

We analyzed the reaction mixture using high-pressure liquid chromatography (HPLC) to determine the fate of the reduced menadione catalyzed by AnNTR (Fig. 3B).

Menadione had a retention time of 14.8 min, and chromatography profiles showed no time-dependent decrease in the substrate peaks. These results suggested that the metabolism of menadione by AnNTR should be a one-electron reductive pathway, in which an unstable semiquinone radical is first generated, and subsequently reoxidized to menadione via redox cycling under aerobic conditions. Back-oxidation of menadione from semiquinone usually generates $O_2^{\bullet-}$ without menadione consumption (34), a process that could explain the nonquantitative changes in menadione observed in the reaction mixture. Another additive agent, FMN, which has a retention time of 13.9 min, was also detected (Fig. 3B). The amounts of FMN after the reaction were not substantially reduced, which should be a property of an electron transfer mediator in redox reactions.

To confirm the generation of $O_2^{\bullet-}$, the reaction products of the menadione reduction were analyzed using EPR spectroscopy after combination with DMPO [5,5-dimethyl-1-pyrroline-N-oxide], an $O_2^{\bullet-}$ trapper (Fig. 3C). This is one of the most widely used methods for the determination of free radicals (35). Without AnNTR, no spectra were detectable in the reaction solution. However, the addition of AnNTR to the reaction mixture produced a strong EPR signal corresponding to the DMPO- $O_2^{\bullet-}$ adduct. This signal was completely quenched by the exogenous superoxide radical scavenging enzyme SOD (Fig. 3C), indicating that menadione-derived $O_2^{\bullet-}$ generation was catalyzed by AnNTR. $O_2^{\bullet-}$ is a highly reactive molecule and can undergo spontaneous dismutation to H_2O_2 , providing the basis for the sensitivity of $\Delta prx A$ and $\Delta cat B$ mutants to menadione (Fig. 2B). To estimate the extent of the oxidative stress attributable to $O_2^{\bullet-}$ -derived H_2O_2 , we measured H_2O_2 levels in the reaction solution. As shown in Fig. 3D, a large amount of H_2O_2 appeared in the AnNTR-catalyzed menadione reduction reaction mixture and was completely decomposed by catalase. Our data demonstrated that AnNTR drives the one-electron metabolism of menadione leading to ROS generation via redox cycling. We proposed that the catalytic process proceeds as follows: AnNTR catalyzes the reduction of menadione to produce semiquinone by accepting one electron from NADPH. The resulting unstable semiquinone is released from AnNTR and quickly reoxidized aerobically to menadione, with concomitant generation of $O_2^{\bullet-}$. Another electron from NADPH participates in the next round of reduction of menadione in the same way. Therefore, the whole reaction appears to be a futile cycle, except for the incessant NADPH consumption and $O_2^{\bullet-}$ generation.

***E. coli* NTR is responsible for cell growth defects caused by menadione.** Recombinant *E. coli* NTR (NfsB) can catalyze menadione to produce $O_2^{\bullet-}$ *in vitro*, a reaction which has been utilized in the development of an $O_2^{\bullet-}$ generation system for biochemical and biomedical applications (9). We compared the efficiency of $O_2^{\bullet-}$ generation catalyzed by bacterial and fungal NTRs and found that the initial velocity of reaction of NfsB was higher than that of AnNTR under the same assay conditions, although the final levels of the product were similar (Fig. 4A). Given the high activity of menadione-dependent $O_2^{\bullet-}$ production catalyzed by purified NfsB, we speculated that NfsB might be an efficient generator of cellular $O_2^{\bullet-}$ in *E. coli*.

To test this hypothesis, the *nfsB* knockout *E. coli* BL21(DE3) ($\Delta nfsB$) was constructed using CRISPR/dCas9-mediated base editing technology (36), and the phenotype was investigated (Fig. 4B). No growth rate difference was observed between the $\Delta nfsB$ mutant and the *E. coli* BL21(DE3) control strain (WT) under normal conditions. Exposure to external menadione at a concentration of 0.3 mM produced more survival stress to the WT than to the $\Delta nfsB$ strain (Fig. 4B), confirming that *E. coli* NfsB had an adverse effect on a menadione detoxification pathway. To investigate possible functional complementarity between the fungal and bacterial NTRs, we heterologously expressed the two NTRs in $\Delta nfsB$ *E. coli* and $\Delta AN2343$ *A. nidulans*, respectively, and characterized their phenotypes. We found that heterologously expressing the two NTRs significantly promoted the menadione sensitivity of both NTR knockout strains (Fig. 4B and C), suggesting that the function of cellular NTRs in inducing cytotoxicity by menadione is evolutionarily conserved.

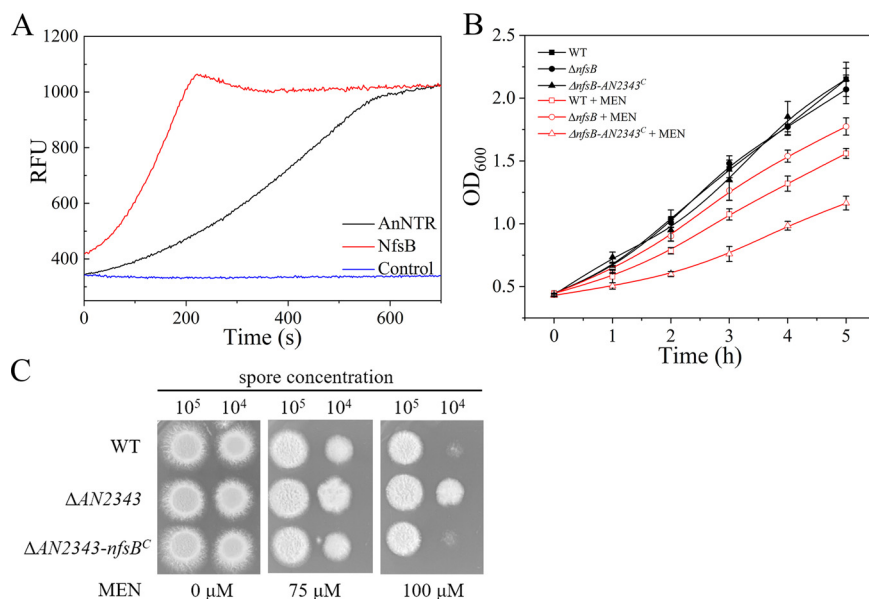


FIG 4 Deleterious effect of NfsB on menadione detoxification in *E. coli*. (A) Comparison of the efficiency of O₂^{•−} generation catalyzed by *A. nidulans* and *E. coli* NTRs. The reaction mixture was the same as that described in Fig. 3A. The reaction was initiated by the addition of 3.6 μM AnNTR or NfsB, respectively. (B) NTRs from either *E. coli* or *A. nidulans* promotes *E. coli* sensitivity to menadione. For the phenotype analysis, *E. coli*-WT (wild-type *E. coli*) and Δ*nfsB* (*E. coli nfsB* disruption) strains were transformed with empty pET32a. The Δ*nfsB*-AN2343^C strain was constructed by introducing the pET32a-AnNTR plasmid into Δ*nfsB* (cross-species complemented with AN2343 in Δ*nfsB*). After induction for 4 h, both strains were diluted to the same concentrations (OD = 0.45) with Luria-Bertani medium (LB) containing 0.8 mM IPTG. Growth curves of both strains in LB with or without 0.3 mM menadione (MEN) were recorded at 1 h intervals at OD₆₀₀. (C) Expression of NfsB in *A. nidulans* ΔAN2343 restored its sensitivity to menadione. Conidia from the WT, ΔAN2343, and ΔAN2343-*nfsB*^C (cross-species complementation of *E. coli nfsB* gene in ΔAN2343) strains with serial dilutions were spotted on minimal media plates with or without the indicated concentrations of menadione, followed by incubation at 37°C for 48 h. The data are the means ± the SD of three independent experiments.

AnNTR has broad substrate specificity but only transcriptionally responds to aromatic compounds. Nitroreductase has been reported to metabolize a wide range of substrates, including nitroaromatic and nitroheterocyclic compounds and quinone derivatives (5, 11, 13, 37). To characterize the substrate specificity of AnNTR, we tested its capability to catalyze the reduction of various nitro-compounds containing different nitro groups in the benzene or heterocyclic rings, as well as the other type of quinone. Activity assays were performed with NADPH as the electron donor and MTT as the chromogenic electron acceptor, and the colored products were quantified. As shown in Table 1, different activity levels were observed for AnNTR with various nitro-compounds, indicating that AnNTR possesses nitroreductase activity *in vitro*. Plumbagin has been reported to be another cytotoxic quinone compound, and is often used as an electrophile of cellular GSH, to produce oxidative stress (38). AnNTR had a clear preference for plumbagin over menadione in reduction activity (Table 1). These results indicated that AnNTR has broad substrate specificity, as is the case for most nitroreductases (11).

We investigated the transcriptional responsiveness of AnNTR gene to the several nitro-compounds listed in Table 1, to further confirm the status of AnNTR as a functional nitroreductase. We found that nitroaromatics such as 2,4,6-trinitrotoluene (TNT) and ethyl *p*-nitrobenzoate (E-PNB) increased the expression of AN2343 by 6- to 50-fold (Fig. 5). AN2343 was less responsive to the nitroheterocyclic derivatives 4-nitroquinoline N-oxide (4-NQO) and metronidazole (MTZ) (Fig. 5). This observation indicated that nitroaromatics are more potent inducers of the AnNTR gene, and the substrate preference is due to the backbone structure rather than the nitro group of the compounds. We next investigated the association between cytotoxicity and AnNTR, using the

TABLE 1 Activity of recombinant AnNTR with different substrates

Substrate	Mean activity ($\Delta A_{590} \text{ min}^{-1} \text{ mg protein}^{-1}$) \pm SD ^a
Nitroaromatics	
2-Nitrotoluene	0.13 \pm 0.09
4-Nitrotoluene	0.09 \pm 0.08
1,3-Dinitrobenzene	0.15 \pm 0.09
2-Chloronitrobenzene	0.09 \pm 0.08
4-Chloronitrobenzene	0.01 \pm 0.00
2-Nitrobenzaldehyde	1.21 \pm 0.09
3-Nitrobenzaldehyde	0.28 \pm 0.08
4-Nitrobenzaldehyde	1.18 \pm 0.09
2-Nitrobenzoate	0.21 \pm 0.09
3-Nitrobenzoate	0.37 \pm 0.08
4-Nitrobenzoate	0.24 \pm 0.08
Ethyl <i>p</i> -nitrobenzoate	0.09 \pm 0.05
4-Nitrophenol	0.27 \pm 0.08
2,4,6-Trinitrotoluene	0.51 \pm 0.03
Chloramphenicol	0.44 \pm 0.22
Nitroheterocyclic derivatives	
Nitrofurantoin	2.20 \pm 0.23
Metronidazole	1.73 \pm 0.22
4-Nitroquinoline N-oxide	3.09 \pm 0.22
Quinones	
Menadione	0.64 \pm 0.22
Plumbagin	7.68 \pm 0.35

^aThe activities of recombinant AnNTR with various nitro- and non-nitro compounds (50 μ M) as the substrates are shown. Functional assays were performed with MTT as a chromogenic electron acceptor and NADPH as an electron donor. The activity was measured as the increase of MTT formazan (590 nm) in the first 0- to 60-s reaction at 25°C. Mean values are given for three replicates after subtraction of substrate blanks.

nitroaromatic compound TNT and the nitroheterocyclic compound 4-NQO. Phenotypic analysis showed that both TNT and 4-NQO produced cytotoxicity in *A. nidulans*, causing growth defects in strains exposed to 40 μ g/ml TNT or 0.3 μ g/ml 4-NQO (see Fig. S2B and C). However, deletion of AnNTR did not alter their susceptibilities to these nitro-compounds, indicating that AnNTR is not the key enzyme in the metabolism of these nitro-compounds, in contrast to findings obtained using bacterial and yeast NTRs (16, 39–42).

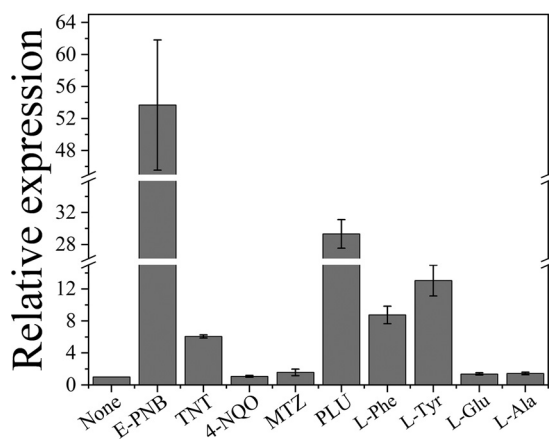


FIG 5 Transcription levels of *AN2343* in response to nitro-compounds and amino acids. After preculture for 16 h in minimal medium, the WT strain was incubated in the presence of a series of nitro-compounds (0.3 mM) or amino acids (5 mM) for 3 h. The relative mRNA expression levels are shown compared to the untreated strain and normalized to *actA*. E-PNB, ethyl *p*-nitrobenzoate; TNT, 2,4,6-trinitrotoluene; 4-NQO, 4-nitroquinoline N-oxide; MTZ, metronidazole; PLU, plumbagin; L-Phe, L-phenylalanine; L-Tyr, L-tyrosine; L-Glu, L-glutamate; L-Ala, L-alanine. The data show the means \pm the SD of three independent experiments.

The significant induction of AnNTR expression triggered by menadione and nitroaromatics, rather than by nitroheterocyclic derivatives, led us to hypothesize that the aromatic nucleus is responsible for the transcriptional upregulation of AnNTR. To test this hypothesis, we investigated the transcriptional responsiveness of *AN2343* to exposure to aromatic amino acids (Fig. 5). *AN2343* expression was upregulated 8-fold after 3 h of incubation with external phenylalanine and 13-fold after incubation with tyrosine. Other amino acids, such as glutamate or alanine, did not evoke this response, confirming our hypothesis that the aromatic group triggers the induction of AnNTR gene expression.

DISCUSSION

It has been suggested that NTRs participate in defense against oxidative stress in cells, acting as ROS-resistant enzymes in many living organisms, including *Aspergillus*. However, our results indicated that although the transcription of NTR from *A. nidulans* is increased in response to menadione-derived ROS, the actual cellular behavior of AnNTR is that of accelerating, rather than inhibiting, ROS generation in the presence of menadione. Subsequent *in vitro* characterization of the menadione reduction catalyzed by AnNTR identified a mechanistic link between ROS generation and the function of AnNTR, in which AnNTR drives the one-electron metabolism of menadione, resulting in $O_2^{\bullet-}$ generation via redox cycling. Our results did not support the contention that NTR is an antioxidant enzyme, protective against quinone toxicity, but indicated that NTR is a key generator of ROS in response to menadione.

Three types of reductases, including NADH ubiquinone oxidase, NADH cytochrome b_5 reductase, and NADPH cytochrome P-450 reductase, have been reported to be responsible for menadione-dependent ROS generation in biological systems (34). We propose that NTR is the fourth menadione reductase capable of generating ROS, based on the performance of AnNTR inside and outside of fungal cells. Moreover, our present data showed that menadione-derived ROS generation activity is not limited to fungal NTR but also occurs in *E. coli* NfsB, suggesting a conserved function among some NTRs. NfsB has been classified as a type I NTR (O_2 -insensitive type) for its two-electron reduction of nitro-compounds. However, acts as a type II (O_2 -sensitive type) NTR when reducing menadione (Fig. 4). The noticeably different reaction mechanisms between the reduction of nitro-compounds and quinones catalyzed by NfsB (11), leading us to suggest that the classification of NTRs based on the biochemical properties of nitro-compound reduction may be not completely adequate to define quinone reductases.

Although there are multiple quinone detoxification enzymes in mammalian, yeast, and bacterial cells, their presence in filamentous fungus is still unconfirmed. Mammalian NAD(P)H:quinone oxidoreductase 1 (NQO1) is known to metabolize quinones to less toxic hydroquinones by two-electron reduction reactions and thus is an endogenous cellular detoxifying enzyme in mammalian cells (34). However, no genes homologous to NQO1 have been found using BLAST against the genomic DNA of *A. nidulans*. The Fqr proteins of *Mycobacterium tuberculosis* catalyze an F_{420} -specific obligate two-electron reduction of endogenous quinones. They thus compete with the one-electron reduction pathway and prevent the formation of harmful cytotoxic semiquinones, protecting mycobacteria against quinone-produced oxidative stress (17). This menadione detoxification pathway probably does not exist in *A. nidulans* due to the absence of the basic components of the reaction systems. Yeast Pst2p has been identified from *S. cerevisiae* cultivated under menadione stress. Pst2p is a nitroreductase-like protein, induced by oxidative stress, whose function is unknown (43, 44). A BLAST search against the *A. nidulans* genomic database identified a protein encoded by *ANO297* that shows high homology to yeast pst2p. *ANO297* is induced by menadione at both transcriptional and translational levels (20, 21), but no further information about this gene has been published. The physiological function of *ANO297* and its corresponding protein will be investigated in the future to determine whether it is a candidate gene for menadione detoxification.

Given that AnNTR accelerates the release of $O_2^{\bullet-}$ from menadione, it is unclear why

TABLE 2 *Aspergillus nidulans* strains used in this study

Strain	Genotype	Source or reference
ABPU1	<i>biA1 pyrG89 wA3 argB2 pyroA4</i>	32
A6	<i>nicA2 veA+</i>	FGSC
Δ AN2343	<i>biA1 pyrG89 wA3 argB2 pyroA4 ΔAN2343::argB</i>	This study
Δ AN2343-com	<i>biA1 pyrG89 wA3 argB2 pyroA4 ΔAN2343::argB AN2343::GFP::pyrG</i>	This study
Δ sodA	<i>biA1 pyrG89 wA3 argB2 pyroA4; ΔsodA::argB</i>	This study
Δ prxA	<i>biA1 pyrG89 wA3 argB2 pyroA4 ΔprxA::argB</i>	29
Δ catB	<i>biA1 pyrG89 wA3; argB2 pyroA4 ΔcatB::argB</i>	Unpublished
Δ AN2343- <i>nfsB</i> ^C	<i>biA1 pyrG89 wA3 argB2 pyroA4 ΔAN2343::argB P_{AN2343}-<i>nfsB</i>-Trpc-pyrG::pyrG</i>	This study

the fungal NTR gene is induced in the presence of menadione. Transcription of AnNTR occurs not only in response to menadione and nitroaromatic compounds but also in response to aromatic amino acids (Fig. 5). We therefore speculated that it is the aromatic nucleus that is responsible for the upregulation of AnNTR. A similar phenomenon has also been observed in the regulation of the bacterial NTR in *Rhodobacter capsulatus*, whose transcription was reported to be upregulated by both nitroaromatic compounds and aromatic amino acids (45). Although *R. capsulatus* NTR (NprA) shows nitroreductase activity with a wide range of nitroaromatic compounds, such as the universal NTRs, NprA may act *in vivo* as a dihydropteridine reductase. In *R. capsulatus*, dihydropteridine reductase catalyzes the reduction of dihydropterine to tetrahydrobiopterin, which is a cofactor for aromatic amino acid hydroxylase, and thus may be involved in the assimilation of aromatic amino acids. Upregulation of NprA increased cell sensitization to some nitroaromatic substrates (45). In view of these data, we speculated that the response of AnNTR gene expression to menadione may be an obligatory misoperation due to the misrecognition of the aromatic amino acids by NTR transcriptional regulation systems. However, the potential involvement of AnNTR in the metabolism of aromatic amino acids requires further experimental confirmation.

MATERIALS AND METHODS

Strains and growth conditions. Fungal strains (Table 2) were grown at 37°C in minimal medium (MM; 10 mM NaNO₃, 10 mM KH₂PO₄, 2 mM MgSO₄, 7 mM KCl, 1% glucose, and 2 ml/liter Hunter's trace metals) supplemented appropriately (0.4 mg/liter biotin, 0.5 g/liter uracil, 0.6 g/liter uridine, and 0.4 mg/liter pyridoxine). *E. coli* DH5 α was used for gene cloning. *E. coli* BL21(DE3) was used for protein expression and phenotype analysis.

Disruption of AnNTR and SodA encoding genes of *A. nidulans*. The disruption primers are listed in Table 3. The AN2343 disruption cassette was constructed to delete the whole AN2343 encoding region using the *A. nidulans* *argB* gene as the selection marker, flanked by 1.1 kb of the 5' and 3' UTRs of the AN2343 gene. PCR was used to amplify the 5'- and 3'-flanking sequences of the AN2343 gene with the specific primer pairs Δ NTR-1/ Δ NTR-2 or Δ NTR-3/ Δ NTR-4. The marker gene *argB* was amplified using *A. nidulans* A6 genomic DNA with the primers *argB*-F and *argB*-R. These DNA fragments were mixed and fused by overlap extension PCR using the nested primers Δ NTR-nest-F and Δ NTR-nest-R. The *sodA* disruption cassette was constructed using the same methods and corresponding primers. The two disruption cassettes were transformed into the ABPU1 strain to obtain Δ AN2343 and Δ sodA mutants, respectively. The resulting disruptants were confirmed using colony PCR with the appropriate primers (Table 3), as shown in Fig. S1.

Disruption of the *nfsB* gene of *E. coli* BL21(DE3). The CRISPER/dCas9-mediated cytidine base editing (CBE) system can be used to inactivate eukaryotic genes through the induction of STOP codons in gene open reading frames (36). Recently, this CBE system was developed in *E. coli* by our lab (unpublished data) and was used in this study to produce the Δ *nfsB* strain. The mutant stain was confirmed by sequencing (see Fig. S5).

Construction of *A. nidulans* strains expressing GFP-tagged AnNTR or *E. coli* NfsB. The corresponding primers are listed in Table 3. The AN2343::gfp cassette was constructed as follows. The marker gene *pyrG* was amplified using PCR with *A. nidulans* A6 genomic DNA and the primers *pyrG*-F and *pyrG*-R. The PCR product was digested with XbaI and then inserted into the XbaI site of pUC19 to construct pUC19-*pyrG*. The *gfp* gene was amplified from the pUC19-*egfp* plasmid produced in our lab using the primers *gfp*-F and *gfp*-R. The DNA fragment, including the native promoter of AN2343 (1-kb 5' UTR of AN2343) and the AN2343 encoding region, was amplified using PCR with *A. nidulans* A6 genomic DNA and the primers NTRgfp-1 and NTRgfp-2. The native terminator region of AnNTR (1-kb 3' UTR of AN2343) was amplified using the primers NTRgfp-3 and NTRgfp-4. The resulting DNA fragments were fused by an overlap PCR using the primers NTRgfp-nest-F and NTRgfp-nest-R, both of which contain the PstI restriction site, and were cloned into pUC19-*pyrG* to produce the GFP-tagged AnNTR expression plasmid

TABLE 3 Primers used in this study

Primer	Gene	Nucleotide sequence (5'–3') ^a
Gene disruption		
ΔNTR-1	<i>AN2343</i>	GAGGAAAGTTCTTGGGATAAGATG
ΔNTR-2		aaaaccgcgaataaagcttAAATAGAAATCATGAAGAGGGGTAG
ΔNTR-3		cgcaatggctgtaggtcgacTTCTGAATAGCATCATAGACGCCG
ΔNTR-4		ACCTTCCACCCCGGAGTCAAC
ΔNTR-nest-F		ATTGGCTATTTTGTCTCGTTGTG
ΔNTR-nest-R		CGCCATAGCAACTCTTGTTCCA
Δ <i>sodA</i> -1	<i>sodA</i>	CAAGTTCGCCGCCGACGCTG
Δ <i>sodA</i> -2		aaaaccgcgaataaagcttACCTGAAAGTGATGTGAGGATGG
Δ <i>sodA</i> -3		cgcaatggctgtaggtcgacGAGAGCTAGGTAGCGCAAACACTGTC
Δ <i>sodA</i> -4		TCTTGAACGACGATCTCCGTTAAC
Δ <i>sodA</i> -nest-F		AAGGTCCAGGCGTAGATGAATGAAC
Δ <i>sodA</i> -nest-R		ACAAGAAGTTCGCGGAGGAATTCG
<i>sodA</i> -check-F		ATGGTCAAGGCTGGTAAGTTGTG
<i>sodA</i> -check-R		TACGCAGCAATACCGATGACACC
<i>argB</i> -F		AAGCTTTATTTTCGCGGTTTTTTG
<i>argB</i> -R		GTCGACCTACAGCCATTGCG
<i>argB</i> -check-3-F		AGTCGTCTAGCCAAGGTAG
<i>argB</i> -check-5-R		AAGTGTCTTCGGAGTCAACC
GFP-tagged AnNTR		
<i>pyrG</i> -F		<u>GCTCTAGAGA</u> ATTTCGATACCTGTGCGAAAG
<i>PyrG</i> -R		<u>GCTCTAGATC</u> AGTGCTTGTCTACCAG
<i>gfp</i> -F		GGAGCTGGTGCAGGCGCTG
<i>gfp</i> -R		TTATTTGTATAGTTCATCCATGCCA
NTR <i>gfp</i> -1		GGGTCAGGTCTCGAACTTTCTAGG
NTR <i>gfp</i> -2		ccagcgcctgcaccagctccCGCGGACTTGCCAAACACCTTG
NTR <i>gfp</i> -3		tgatgaactatacaataaATTCTGAATAGCATCATAGACGCCG
NTR <i>gfp</i> -4		GCAAGTCTCCATTATCAAGCCCTG
NTR <i>gfp</i> -nest-F		<u>AACTGCAGTT</u> GTAATATGCCATAATACAGTGC
NTR <i>gfp</i> -nest-R		<u>AACTGCAGATT</u> CTATCCCTACAATCCTTCCCTC
P_{AN2343}-<i>nfsB</i>		
P _{AN2343} -F		TCTAGAGTCGACCTGCAGACTTGCAATTGAACCAGTTGGTT
P _{AN2343} -R		ATCCATTGTGACTTGCGCTGCTAGAGAC
<i>trpC</i> -F		CCTTAACCGAAGTGTAATGATTTAATAGCTCCATGTCAACAAG
<i>trpC</i> -R		GCTATGACCATGATTACGCCAAAGAAGGATTACCTTAAACAAGTG
<i>nfsB</i> -F		CAGCGCAAGTCACAATGGATATCATTTTCTGTCGCCTTA
<i>nfsB</i> -R		TCATTACACTTCGGTTAAGGTGATGTTTT
pUC- <i>pyrG</i> -F		GGCGTAATCATGGTCAATAGC
pUC- <i>pyrG</i> -R		CTGCAGGTCGACTCTAGAG
q-RT-PCR		
q-RT-NTR-F	<i>AN2343</i>	CGCTCTCAAGGACATCAAGG
q-RT-NTR-R		AAGTACTGAGACATGGCATTGG
q-RT- <i>catB</i> -F	<i>catB</i>	GGAAAGCTCAGCAAATTTCTCG
q-RT- <i>catB</i> -R		CACGTTAAGCTCCCACTCAG
q-RT- <i>sodA</i> -F	<i>sodA</i>	GATAAGCTGATCAAGCTCATTGG
q-RT- <i>sodA</i> -R		GCCAAGGTCATCAGTACCAG
q-RT- <i>prxA</i> -F	<i>prxA</i>	CCCCGCTGACGTTGTCTTC
q-RT- <i>prxA</i> -R		GAGGGCGAAGAGGATGACC
q-RT- <i>actA</i> -F	<i>actA</i>	GAAGTCTACGAACTGCCTGATG
q-RT- <i>actA</i> -R		GACCAAGAACGCTGGGCTGG
Gene cloning		
AnNTR-F	<i>AN2343</i>	CCGG <u>AATTCAT</u> GGTTCGAGTTCAAGAACCCCGC
AnNTR-R		ATAAGAAT <u>GCGGCCGCTT</u> ACGCGGACTTGCCAAACACC
<i>nfsB</i> -F'	<i>nfsB</i>	CGCG <u>GATCCAT</u> GGATATCATTTTCTGTCGCCTTAAAG
<i>nfsB</i> -R'		CCC <u>AGCTTTT</u> ACACTTCGGTTAAGGTGATGTTTTGC
<i>trxA</i> -F	<i>trxA</i>	CATCATCATCATTAATCTGGTCTGGTGCCA
<i>trxA</i> -R		TGGCACCAGACCAGATTAATGATGATGATGATG

^aAll restriction enzymes sites in the primer sequences are underlined. Sections indicated by lowercase letters were designed to overlap the 5'- and 3'-terminal sequences of the marker and GFP genes, respectively.

pNTR gfp . The pNTR gfp plasmid was transformed into the $\Delta AN2343$ strain to obtain a strain harboring GFP-tagged AnNTR.

A strain expressing NfsB in $\Delta AN2343$ was constructed as follows. The DNA fragments containing the AN2343 native promoter (2-kb 5' UTR of AN2343) and the Trpc terminator were amplified using PCR with A6 genomic DNA and two primer pairs, P_{AN2343-F}/P_{AN2343-R} and *trpC-F*/*trpC-R*. The *nfsB* gene was amplified using the primers *nfsB-F* and *nfsB-R*. pUC19-*pyrG* was linearized using PCR with the primers pUC-*pyrG-F* and pUC-*pyrG-R*. These DNA fragments were connected using In-Fusion HD cloning kits (Takara Bio, Shiga, Japan). The resultant plasmid, pP_{AN2343-nfsB-Trpc-pyrG}, was transformed into the $\Delta AN2343$ strain to obtain a strain expressing *E. coli* NfsB.

Fluorescence microscopy. *A. nidulans* conidiospores (5×10^4) were inoculated onto a glass-bottom cell culture dish (NEST Biotechnology, Wuxi, China) dipped in 200 μ l of MM medium and grown at 37°C for 12 h. The hyphae were then washed twice with phosphate-buffered saline (PBS; pH 7.4) after removal of the MM medium and observed using confocal laser scanning microscopy (TCS SP8; Leica, Wetzlar, Germany). To examine the O₂^{•-} produced by menadione, 300 μ M menadione was added to 200 μ l of MM for 1 h after 12 h of cultivation, followed by treatment with 10 μ M dihydroethidium (DHE) and incubation at 37°C for 30 min. Subsequently, dishes with attached mycelia were washed twice with PBS (pH 7.4), and the intracellular O₂^{•-} levels were monitored by the formation of ethidium from DHE. The fluorescence of the GFP and the O₂^{•-} specific products for DHE were imaged using excitation with a 488-nm laser and a 405-nm laser, respectively.

Quantitative PCR. Strains were cultured in MM for 16 h and then treated with the indicated concentrations of various compounds for 3 h. Mycelia were harvested by filtration, and total RNA was extracted using EZ-10 DNAaway RNA Mini-Prep kits (Sangon, China). cDNAs were reverse transcribed using ReverTra Ace qPCR RT Master Mix with gDNA remover (Toyobo Co., Ltd., Osaka, Japan). The primer pairs q-RT-NTR-F/q-RT-NTR-R, q-RT-*catB*-F/q-RT-*catB*-R, q-RT-*sodA*-F/q-RT-*sodA*-R, q-RT-*prxA*-F/q-RT-*prxA*-R, and q-RT-*actA*-F/q-RT-*actA*-R (Table 3) were used to amplify the AN2343, *catB*, *sodA*, *prxA*, and *actA* genes, respectively. The relative mRNA levels were normalized to that of *actA*, which was used as a reference gene.

Measurement of O₂^{•-} and H₂O₂. Electron paramagnetic resonance (EPR) was used to measure the O₂^{•-} generated by the AnNTR-catalyzed menadione reduction. All EPR spectra were recorded at room temperature on a Bruker BioSpin EMX-8/2.7 (Bruker Corporation, Billerica, MA) at 9.8 GHz with a 100-kHz modulation frequency and a 1.0-G modulation amplitude. The reaction mixture for EPR analysis was 0.5 ml sodium phosphate buffer (50 mM [pH 7.4]) containing AnNTR (1.5 μ g), menadione (50 μ M), NADPH (100 μ M), diethylenetriaminepentaacetic acid (DTPA; 100 μ M), FMN (10 μ M), and DMPO (40 mM). The reaction was initiated by the addition of the enzyme and quickly transferred into a quartz capillary. H₂O₂, as a disproportionation reaction product of O₂^{•-} from the above-mentioned reaction, was analyzed using hydrogen peroxide assay kits (Beyotime Biotech, Haimen, China), and the absorbance was measured at 540 nm using a U-5100 spectrophotometer (Hitachi, Tokyo, Japan). The rates of O₂^{•-} generation catalyzed by AnNTR and *E. coli* NfsB were assayed in a reaction mixture containing a final volume of 0.5 ml of 50 mM sodium phosphate buffer (pH 7.4), 400 μ M NADPH, 100 μ M DTPA, 10 μ M FMN, 200 μ M menadione, 50 μ M DHE, and 3.6 μ M AnNTR or NfsB. The fluorescence of DHE oxidized by O₂^{•-} was monitored by using a fluorescence spectrophotometer (F-4600; Hitachi).

The intracellular O₂^{•-} levels were measured as follows. Approximately 1×10^8 conidiospores of the control and $\Delta AN2343$ strains were inoculated into 250-ml Erlenmeyer flasks containing 100 ml of medium and cultured at 37°C for 16 h at 200 rpm. All mycelium samples were filtered using a textile filter (Miraclon; Calbiochem, San Diego, CA) and transferred immediately into 100 ml of medium with or without 0.8 mM menadione. After menadione treatment for 6 h, 10 μ M DHE was added for 1 h, and the fluorescence was tested. Mycelia were harvested by filtration, immediately ground into a powder with liquid nitrogen, and then suspended in 50 mM sodium phosphate buffer (pH 7.4). The supernatant of the disrupted mycelia was used for fluorescence detection.

Cloning, expression, and purification of AnNTR and *E. coli* NfsB. The cDNA of AnNTR was subcloned using the primers AnNTR-F and AnNTR-R (Table 3). The PCR-amplified product was digested using the appropriate restriction enzymes and inserted into pET32a. The *nfsB* gene was amplified with the primers *nfsB-F'* and *nfsB-R'* (Table 3) and subcloned into pET32a to create the overexpression vector pET32a-*nfsB*. To express the TrxA tag (13.2 kDa), a stop codon (TAA) was introduced at the multiple-cloning site just before the thrombin site in the empty pET32a by using site-directed mutagenesis with the primers *trxA-F* and *trxA-R* (Table 3). *E. coli* BL21(DE3) cells containing each plasmid were cultured at 37°C in the presence of 50 μ g/ml ampicillin to an optical density (OD) of 0.5. Protein expression was induced by the addition of 0.5 mM IPTG (isopropyl-1-thio- β -D-galactopyranoside) for 12 h at 30°C. Recombinant AnNTR, NfsB, and TrxA were purified from these fractions using a HisTrap FF column (GE Healthcare, Chicago, IL) and characterized using SDS-PAGE analysis.

Enzyme assays. The nitro-compound and quinone reductase activities of recombinant AnNTR were measured spectrophotometrically by monitoring MTT reduction at 590 nm, as previously described (33). The reaction mixture contained 0.5 ml of sodium phosphate buffer (50 mM [pH 7.4]), NADPH (100 μ M), DTPA (100 μ M), FMN (10 μ M), MTT (0.5 mM), various substrates (50 μ M), and AnNTR (1.5 μ g). After subtraction of the substrate blanks, the activities were measured as the change in absorbance at 590 nm (ΔA_{590}).

Aconitase activity was detected using Cis-Aconitase (ACO) activity detection kits (Solarbio Life Sciences, Beijing, China). The production of 1 nmol of *cis*-aconitate per min per mg of protein was defined as 1 U of aconitase activity.

Menadione reduction products. The products of menadione reduction were analyzed using HPLC (Agilent 1260; Agilent Technologies, Santa Clara, CA) with a reversed-phase column (TSKgel ODS-100V,

4.6 × 15 cm; Tosoh Co., Ltd., Tokyo, Japan). The HPLC conditions were as follows. The column was pre-equilibrated with 95% B for 20 min; 0 to 15 min, using a linear gradient from 95% A to 5% A; 15 to 17 min, a linear gradient from 5% A to 95% A; 17 to 20 min, constant with 95% A; the flow rate was maintained at 0.3 ml/min, and the eluent was monitored using a UV detector at 300 nm. Solvent A was 0.1% formic acid in H₂O, and solvent B was 0.1% formic acid in acetonitrile.

Data availability. All necessary data required to assess our findings are available in this manuscript or its supplementary materials.

SUPPLEMENTAL MATERIAL

Supplemental material is available online only.

SUPPLEMENTAL FILE 1, PDF file, 0.5 MB.

ACKNOWLEDGMENTS

This study was funded by the International S&T Innovation Cooperation Key Project (2017YFE0129600), the National Natural Science Foundation of China (21672065, 22077032, and 21636003), the National Major Science and Technology Projects of China (2019ZX09739001), the Fundamental Research Funds for the Central Universities (22221818014), and the 111 Project (B18022).

REFERENCES

- West AP, Shadel GS, Ghosh S. 2011. Mitochondria in innate immune responses. *Nat Rev Immunol* 11:389–402. <https://doi.org/10.1038/nri2975>.
- Schieber M, Chandel NS. 2014. ROS function in redox signaling and oxidative stress. *Curr Biol* 24:R453–R462. <https://doi.org/10.1016/j.cub.2014.03.034>.
- Dharmaraja AT, Chakrapani H. 2014. A small molecule for controlled generation of reactive oxygen species (ROS). *Org Lett* 16:398–401. <https://doi.org/10.1021/ol403300a>.
- Liu Z, Deeth RJ, Butler JS, Habtemariam A, Newton ME, Sadler PJ. 2013. Reduction of quinones by NADH catalyzed by organoiridium complexes. *Angew Chem Int Ed Engl* 52:4194–4197. <https://doi.org/10.1002/anie.201300747>.
- Haas J, Schätzle MA, Husain SM, Schulz-Fincke J, Jung M, Hummel W, Müller M, Lüdeke S. 2016. A quinone mediator drives oxidations catalysed by alcohol dehydrogenase-containing cell lysates. *Chem Commun (Camb)* 52:5198–5201. <https://doi.org/10.1039/c5cc10316a>.
- Uchiyama N, Kabututu Z, Kubata BK, Kiuchi F, Ito M, Nakajima-Shimada J, Aoki T, Ohkubo K, Fukuzumi S, Martin SK, Honda G, Urade Y. 2005. Antichagasic activity of komaroviquinone is due to generation of reactive oxygen species catalyzed by *Trypanosoma cruzi* old yellow enzyme. *Antimicrob Agents Chemother* 49:5123–5126. <https://doi.org/10.1128/AAC.49.12.5123-5126.2005>.
- Radman M. 2016. Protein damage, radiation sensitivity, and aging. *DNA Repair (Amst)* 44:186–192. <https://doi.org/10.1016/j.dnarep.2016.05.025>.
- Hassan GS. 2013. Menadione. *Profiles Drug Subst Excip Relat Methodol* 38:227–313. <https://doi.org/10.1016/B978-0-12-407691-4.00006-X>.
- Singh SK, Husain SM. 2018. A redox-based superoxide generation system using quinone/quinone reductase. *Chembiochem* 19:1657–1663. <https://doi.org/10.1002/cbic.201800071>.
- Iyanagi T, Yamazaki I. 1970. One-electron-transfer reactions in biochemical systems. V. Difference in the mechanism of quinone reduction by the NADH dehydrogenase and the NAD(P)H dehydrogenase (DT-diaphorase). *Biochim Biophys Acta* 216:282–294. [https://doi.org/10.1016/0005-2728\(70\)90220-3](https://doi.org/10.1016/0005-2728(70)90220-3).
- Roldán MD, Pérez-Reinado E, Castillo F, Moreno-Vivián C. 2008. Reduction of polynitroaromatic compounds: the bacterial nitroreductases. *FEMS Microbiol Rev* 32:474–500. <https://doi.org/10.1111/j.1574-6976.2008.00107.x>.
- Rau J, Stolz A. 2003. Oxygen-insensitive nitroreductases *NfsA* and *NfsB* of *Escherichia coli* function under anaerobic conditions as lawsone-dependent Azo reductases. *Appl Environ Microbiol* 69:3448–3455. <https://doi.org/10.1128/AEM.69.6.3448-3455.2003>.
- Pérez-Reinado E, Blasco R, Castillo F, Moreno-Vivián C, Roldán MD. 2005. Regulation and characterization of two nitroreductase genes, *nprA* and *nprB*, of *Rhodobacter capsulatus*. *Appl Environ Microbiol* 71:7643–7649. <https://doi.org/10.1128/AEM.71.12.7643-7649.2005>.
- Mostertz J, Scharf C, Hecker M, Homuth G. 2004. Transcriptome and proteome analysis of *Bacillus subtilis* gene expression in response to superoxide and peroxide stress. *Microbiology (Reading)* 150:497–512. <https://doi.org/10.1099/mic.0.26665-0>.
- Streker K, Freiberg C, Labischinski H, Hacker J, Ohlsen K. 2005. *Staphylococcus aureus* NfrA (SA0367) is a flavin mononucleotide-dependent NADPH oxidase involved in oxidative stress response. *J Bacteriol* 187:2249–2256. <https://doi.org/10.1128/JB.187.7.2249-2256.2005>.
- de Oliveira IM, Zanotto-Filho A, Moreira JC, Bonatto D, Henriques JA. 2010. The role of two putative nitroreductases, F₄₂₀p and Hbn1p, in the oxidative stress response in *Saccharomyces cerevisiae*. *Yeast* 27:89–102.
- Gurumurthy M, Rao M, Mukherjee T, Rao SP, Boshoff HI, Dick T, Barry CE, III, Manjunatha UH. 2013. A novel F₄₂₀-dependent anti-oxidant mechanism protects *Mycobacterium tuberculosis* against oxidative stress and bactericidal agents. *Mol Microbiol* 87:744–755. <https://doi.org/10.1111/mmi.12127>.
- Mascotti ML, Juri Ayub M, Fraaije MW. 2021. On the diversity of F₄₂₀-dependent oxidoreductases: a sequence- and structure-based classification. *Proteins* <https://doi.org/10.1002/prot.26170>.
- Leiter É, Bálint M, Miskei M, Orosz E, Szabó Z, Pócsi I. 2016. Stress tolerances of nullmutants of function-unknown genes encoding menadione stress-responsive proteins in *Aspergillus nidulans*. *J Basic Microbiol* 56: 827–833. <https://doi.org/10.1002/jobm.201500500>.
- Pócsi I, Miskei M, Karányi Z, Emri T, Ayoubi P, Pusztahelyi T, Balla G, Prade RA. 2005. Comparison of gene expression signatures of diamide, H₂O₂ and menadione exposed *Aspergillus nidulans* cultures-linking genome-wide transcriptional changes to cellular physiology. *BMC Genomics* 6:182. <https://doi.org/10.1186/1471-2164-6-182>.
- Pusztahelyi T, Klement E, Szajli E, Klem J, Miskei M, Karányi Z, Emri T, Kovács S, Orosz G, Kovács KL, Medzihradszky KF, Prade RA, Pócsi I. 2011. Comparison of transcriptional and translational changes caused by long-term menadione exposure in *Aspergillus nidulans*. *Fungal Genet Biol* 48: 92–103. <https://doi.org/10.1016/j.fgb.2010.08.006>.
- Chauhan N, Latge JP, Calderone R. 2006. Signalling and oxidant adaptation in *Candida albicans* and *Aspergillus fumigatus*. *Nat Rev Microbiol* 4: 435–444. <https://doi.org/10.1038/nrmicro1426>.
- Li Q, Bai Z, O'Donnell A, Harvey LM, Hoskisson PA, McNeil B. 2011. Oxidative stress in fungal fermentation processes: the roles of alternative respiration. *Biotechnol Lett* 33:457–467. <https://doi.org/10.1007/s10529-010-0471-x>.
- Toledano M, Delaunay A, Biteau B, Spector D, Azevedo D. 2004. Oxidative stress responses in yeast, p 241–303. *In* Hohmann S, Mager WH (ed), *Yeast stress responses*. Springer, Berlin, Germany.
- Pócsi I, Prade RA, Penninckx MJ. 2004. Glutathione, altruistic metabolite in fungi. *Adv Microb Physiol* 49:1–76. [https://doi.org/10.1016/S0065-2911\(04\)49001-8](https://doi.org/10.1016/S0065-2911(04)49001-8).
- Shertzer HG, Låstbom L, Sainsbury M, Moldéus P. 1992. Menadione-mediated membrane fluidity alterations and oxidative damage in rat hepatocytes. *Biochem Pharmacol* 43:2135–2141. [https://doi.org/10.1016/0006-2952\(92\)90172-F](https://doi.org/10.1016/0006-2952(92)90172-F).

27. Wang Y, Branicky R, Noë A, Hekimi S. 2018. Superoxide dismutases: Dual roles in controlling ROS damage and regulating ROS signaling. *J Cell Biol* 217:1915–1928. <https://doi.org/10.1083/jcb.201708007>.
28. Leiter É, Park HS, Kwon NJ, Han KH, Emri T, Oláh V, Mészáros I, Dienes B, Vincze J, Csernoch L, Yu JH, Pócsi I. 2016. Characterization of the *aodA*, *dnmA*, *mnSOD*, and *pimA* genes in *Aspergillus nidulans*. *Sci Rep* 6:20523. <https://doi.org/10.1038/srep20523>.
29. Xia Y, Yu H, Zhou Z, Takaya N, Zhou S, Wang P. 2018. Peroxiredoxin system of *Aspergillus nidulans* resists inactivation by high concentration of hydrogen peroxide-mediated oxidative stress. *J Microbiol Biotechnol* 28:145–156. <https://doi.org/10.4014/jmb.1707.07024>.
30. Mendoza-Martínez AE, Lara-Rojas F, Sánchez O, Aguirre J. 2017. NapA mediates a redox regulation of the antioxidant response, carbon utilization and development in *Aspergillus nidulans*. *Front Microbiol* 8:516. <https://doi.org/10.3389/fmicb.2017.00516>.
31. Kawasaki L, Aguirre J. 2001. Multiple catalase genes are differentially regulated in *Aspergillus nidulans*. *J Bacteriol* 183:1434–1440. <https://doi.org/10.1128/JB.183.4.1434-1440.2001>.
32. Zhou S, Narukami T, Nameki M, Ozawa T, Kamimura Y, Hoshino T, Takaya N. 2012. Heme-biosynthetic porphobilinogen deaminase protects *Aspergillus nidulans* from nitrosative stress. *Appl Environ Microbiol* 78:103–109. <https://doi.org/10.1128/AEM.06195-11>.
33. Muller J, Rout S, Leitsch D, Vaithilingam J, Hehl A, Muller N. 2015. Comparative characterization of two nitroreductases from *Giardia lamblia* as potential activators of nitro compounds. *Int J Parasitol Drugs Drug Resist* 5:37–43. <https://doi.org/10.1016/j.ijpddr.2015.03.001>.
34. Criddle DN, Gillies S, Baumgartner-Wilson HK, Jaffar M, Chinje EC, Passmore S, Chvanov M, Barrow S, Gerasimenko OV, Tepikin AV, Sutton R, Petersen OH. 2006. Menadione-induced reactive oxygen species generation via redox cycling promotes apoptosis of murine pancreatic acinar cells. *J Biol Chem* 281:40485–40492. <https://doi.org/10.1074/jbc.M607704200>.
35. Sealy RC, Swartz HM, Olive PL. 1978. Electron spin resonance-spin trapping: detection of superoxide formation during aerobic microsomal reduction of nitro-compounds. *Biochem Biophys Res Commun* 82:680–684. [https://doi.org/10.1016/0006-291X\(78\)90928-2](https://doi.org/10.1016/0006-291X(78)90928-2).
36. Billon P, Bryant EE, Joseph SA, Nambiar TS, Hayward SB, Rothstein R, Ciccía A. 2017. CRISPR-mediated base editing enables efficient disruption of eukaryotic genes through induction of STOP codons. *Mol Cell* 67:1068–1079.e4. <https://doi.org/10.1016/j.molcel.2017.08.008>.
37. Nokhbeh MR, Boroumandi S, Pokorny N, Koziarz P, Paterson ES, Lambert IB. 2002. Identification and characterization of SnrA, an inducible oxygen-insensitive nitroreductase in *Salmonella enterica* serovar Typhimurium TA1535. *Mutat Res* 508:59–70. [https://doi.org/10.1016/S0027-5107\(02\)00174-4](https://doi.org/10.1016/S0027-5107(02)00174-4).
38. Castro FA, Mariani D, Panek AD, Eleutherio EC, Pereira MD. 2008. Cytotoxicity mechanism of two naphthoquinones (menadione and plumbagin) in *Saccharomyces cerevisiae*. *PLoS One* 3:e3999. <https://doi.org/10.1371/journal.pone.0003999>.
39. Bang SY, Kim JH, Lee PY, Bae KH, Lee JS, Kim PS, Lee DH, Myung PK, Park BC, Park SG. 2012. Confirmation of Frm2 as a novel nitroreductase in *Saccharomyces cerevisiae*. *Biochem Biophys Res Commun* 423:638–641. <https://doi.org/10.1016/j.bbrc.2012.05.156>.
40. Mermod M, Mourlane F, Waltersperger S, Oberholzer AE, Baumann U, Solioz M. 2010. Structure and function of CinD (YtjD) of *Lactococcus lactis*, a copper-induced nitroreductase involved in defense against oxidative stress. *J Bacteriol* 192:4172–4180. <https://doi.org/10.1128/JB.00372-10>.
41. Salamanca-Pinzón SG, Camacho-Carranza R, Hernández-Ojeda SL, Espinosa-Aguirre JJ. 2006. Nitro-compound activation by cell-free extracts of nitroreductase-proficient *Salmonella* Typhimurium strains. *Mutagenesis* 21:369–374. <https://doi.org/10.1093/mutage/gel042>.
42. Carroll CC, Warnakulasuriyarachchi D, Nokhbeh MR, Lambert IB. 2002. *Salmonella* Typhimurium mutagenicity tester strains that overexpress oxygen-insensitive nitroreductases *nfsA* and *nfsB*. *Mutat Res* 501:79–98. [https://doi.org/10.1016/S0027-5107\(02\)00018-0](https://doi.org/10.1016/S0027-5107(02)00018-0).
43. Kim IS, Yun HS, Kwak SH, Jin IN. 2007. The physiological role of CPR1 in *Saccharomyces cerevisiae* KNU5377 against menadione stress by proteomics. *J Microbiol* 45:326–332.
44. Lee J, Godon C, Lagniel G, Spector D, Garin J, Labarre J, Toledano MB. 1999. Yap1 and Skn7 control two specialized oxidative stress response regulons in yeast. *J Biol Chem* 274:16040–16046. <https://doi.org/10.1074/jbc.274.23.16040>.
45. Pérez-Reinado E, Roldán MD, Castillo F, Moreno-Vivián C. 2008. The NprA nitroreductase required for 2,4-dinitrophenol reduction in *Rhodobacter capsulatus* is a dihydropteridine reductase. *Environ Microbiol* 10:3174–3183. <https://doi.org/10.1111/j.1462-2920.2008.01585.x>.